HIGH-PRESSURE DIE CASTS GATING SYSTEM NUMERICAL DESIGN METHODOLOGY ASSESSMENT WITH REGARD TO HYDRODYNAMIC CONDITIONS IN THE MELT FLOW

MICHAELA MAJERNIKOVA[1], JAN MAJERNIK[1,2], MARTIN PODARIL[1], JAN KOLINSKY[1]

[1]The Institute of Technology and Business in Ceske Budejovice, Faculty of Technology, Department of Mechanical Engineering, Ceske Budejovice, Czech Republic

[2] Faculty of Agriculture and Technology, University of South Bohemia in Ceske Budejovice, Ceske Budejovice, Czech Republic

DOI: 10.17973/MMSJ.2025_03_2024119

e-mail: jmajernik@jcu.cz

High-pressure die casts exhibit a certain amount of porosity, which can reduce their mechanical properties. One of the options for maintaining the porosity of casts at a low value is the correct gating system design. Presented contribution is based on the conclusions of the "Methodology assessment of the gating system numerical design of high-pressure die casting with regard to the material applicability" contribution. Individual numerical design methods gave different dimensions and cross-sections for the runners. Based on the assumption of a Reynolds number Re modification when altering the hydraulic cross-sections of the runners, it is possible to conclude that the nature of the melt flow in the runners is also shifting. The presented contribution aims to analytically determine the hydrodynamic conditions in the melt with different designs of the gating systems, determine the filling mode of the mold cavity and subsequently, using a simulation program, to determine the share of gas entrapment in the casts volume. At the end of the contribution, assumptions are deduced about the mechanism of gas entrapment in the casts volume.

KEYWORDS

HPDC, gating systems design, aluminum casts, Reynolds number, metal flow characteristic

1 INTRODUCTION

High-pressure die casting (HDPC) technology is gaining ground in the production of high-quality casts for a wide range of industries. It holds this position mainly due to the production of parts with little or no finishing operations [Cao 2020, Tavodova 2022]. High-pressure die casts are characterized by high geometric accuracy, good mechanical properties and low price. Good mechanical properties of casts are related to their fine-grained structure, which is formed by the supercooling of the melt in contact with the relatively cold wall of the mold cavity, however, casting defects related to the porosity and the presence of the gases in melt significantly affect the quality of casts [Zhao 2018, Dybalska 2021]. Identification of the porosity type in casts is often difficult due to the mold cavity filling mechanism, runners melt flow and the simultaneous crystallization and shrinkage during solidification and cooling [Otsuka 2014]. Inhomogeneities in the casts volume by shrinkage are principally a function of casts material, the mold material and the temperature field during solidification of the casts [Novakova 2017, Bolibruchova 2019]. Metal molds facilitate intensive heat removal from the melt and its faster solidification, which leads to a smaller distance between the main axes of the dendritic cells and a fine-grained structure is formed. A larger distance between the main axes of the dendritic cells facilitates the melt segregation during a lower cooling rate and allows the formation of inter-dendritic porosity [Vlach 2022].

The introduction of gases into casts and the reduction of gas porosity are possible by appropriate melting control and melt treatment, setting technological parameters in the casting cycle and last but not least, by the correct gating system design [Uhricik 2017, Gaspar 2019]. In the field of casting, the gating system has an important influence on the flow field, heat transfer and solidification process. The reasonable gating system design and the setting of the casts parameters, as well as whether the mechanical properties of the key parts can meet the actual needs, have become not only the main part in the production of high-quality casts, but also a popular research problem in the field of material processing [Duan 2023]. It is advisable to design the gating system and the runners in such a way that the smoothest possible melt flow is achieved without the formation of turbulence and thus the gas entrapment by the melt and their subsequent transport into the cast volume. In general, in high-pressure die casting technology, it is not possible to maintain the laminar flow in runners due to the high melt flow velocities [Kuznetsov 2020]. Therefore, it is advisable to design the cross-section and shape of the channels in such a way that the turbulent flow is kept as low as possible. Turbulent molten metal filling during casting leads to creation of bi-layers, porosity and oxide inclusions, which leads to poor mechanical properties and high reject rates of casts. Therefore, it is important to understand the metal flow when passing through the mold gating system, i.e. the hydrodynamics of the casting, in order to eliminate the casting defects [Majernik 2019, Serak 2020, Bate 2023]. A suitable indicator for this concept is the Reynolds number Re, the degree of melt flow turbulence in the runners. The Reynolds number Re is the ratio of inertial forces to viscous forces in the melt. Studies [Damle 1996, Sahai 1996] show that by comparing the Reynolds number in reduced water models for casting, a reliable metal-water analogy could be achieved.

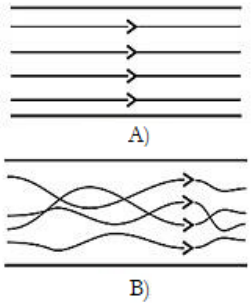

Figure 1. Principle diagram of the melt flow type

In general, we distinguish two types of the flow in liquids (and according to [Damle 1996, Sahai 1996] also melts), namely laminar flow (Fig. 1 A) and turbulent flow (Fig. 1 B).

In laminar flow, the melt flows without mixing of partial streams at low velocities. Turbulent flow is characterized by mixing of partial streams of the melt at higher velocities [Ragan 2007]. Reynolds number Re can be characterized by:

$$Re = \frac{v*d}{\upsilon} \quad (1)$$

Where:

Re – Reynolds number [-],

v – melt flow velocity [ms^{-1}],

d – diameter of the pipe in which the melt flows, or hydraulic diameter of pipe [m],

υ – kinematic viscosity [m^2s^{-1}].

The range is defined by the critical Reynolds number Re_{crit} = 2320, where laminar flow is defined as $Re < Re_{crit}$ and turbulent flow as $Re > Re_{crit}$.

It is important to emphasize that when filling the mold cavity, the melt flow face is more important than the melt flow character [Pasko 2014, Gaspar 2016]. In conventional high-pressure die casting, we distinguish between planar, non-planar and dispersed flow in terms of the melt flow face (Fig. 2).

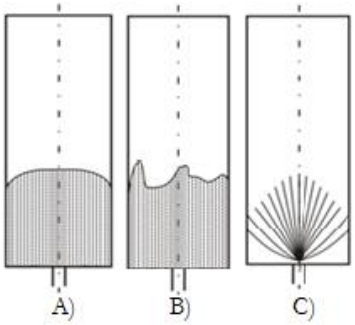

Figure 2. Character of melt flow face

In planar flow (Fig. 2 A), the flow face is continuous, regular over the entire width of the mold cavity, no gas entrapment when filling the mold cavity at low velocity. In non-planar flow (Fig. 2 B), the melt flow face is irregular in a narrower range than the width of the mold cavity, gas entrapment is present when filling the mold cavity at higher velocities. In dispersed flow (Fig. 2 C), a dispersed mixture of liquid metal and gas is formed. In conventional high-pressure die casting, dispersed flow occurs most often in thin-walled casts, non-planar flow occurs in thicker casts, and planar flow occurs only in exceptional cases [Ragan 2007, Majidi 2019].

The basics of the mold cavity alloy filling process theory during the high pressure die casting were developed by researchers Frommer and Brandt [Ragan 2007, Ruzbarsky 2014]. It is stated that it is necessary to distinguish two basic possibilities of the mold filling process, determined by the ratio of the gate cross-section and the cast cross-section:

a) $$\frac{S_G}{S_C} < \mathbf{0.25} \quad (2)$$

b) $$\frac{S_G}{S_C} > \mathbf{0.25} \quad (3)$$

Where:

S_G – gate cross-section corresponding to the filling stream cross-section [m^2],

S_C – cross-section of the mold cavity in which the gate is inserted [m^2].

In the case of filling according to (2), the mold cavity filling is according to Frommer (Fig. 3), where the melt stream moving at high velocity hits the wall of the mold cavity opposite to the gate. The metal stream is dispersed onto the vertical mold cavity walls and travels along them back to the gate, where the pulsations are gradually calmed down [Ragan 2007, Ruzbarsky 2014].

In the case of ratio according to (3), the metal stream moving at low velocity disperses after leaving the gate and mold cavity is filled from the gate to the distant parts of the mold cavity according to Fig. 4. Mold cavity filling proceeds according to Brandt [Ragan 2007, Ruzbarsky 2014].

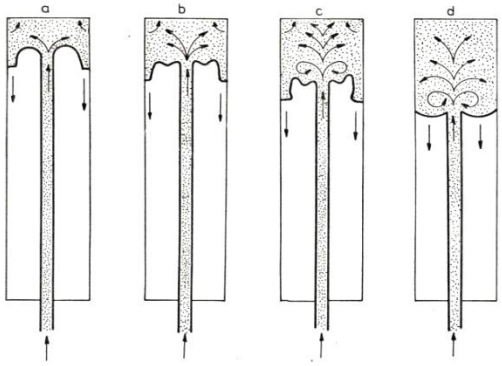

Figure 3. The mold cavity filling process according to Frommer

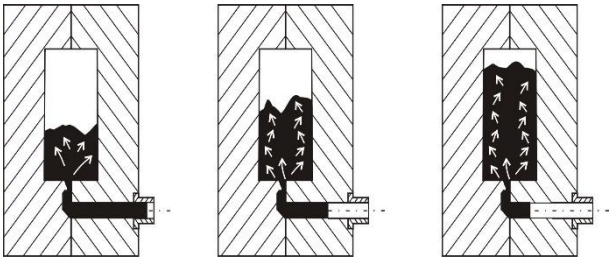

Figure 4. The mold cavity filling process according to Brandt

Based on observations and the utilization of the water-melt analogy, it is possible to express the opinion that with a decreasing ratio according to relations (2) and therefore with a decreasing gate area while maintaining a constant mold cavity cross-sectional area, the emergence of a disperse melt flow will be more pronounced in the mold cavity [Majidi 2019, Cao 2019]. The presented contribution deals with the evaluation of hydrodynamic conditions in the melt flow during the passage through the gating system of a high-pressure die casting mold depending on the gating system numerical design method dimensions modification. The methodology for the gating system design and the numerical designs of the gating system geometry proposed according to it are taken from the article Methodology assessment of the gating system numerical design of high-pressure die casting with regard to the material applicability [Majernikova 2024]. From the article arises that when using various mathematical formulations to determine the gate area and the method to determine the filling time of mold cavity, five variants of the gating systems with different geometric dimensions and characteristics were determined and designed. The design methodology was assessed in article [Majernikova 2024] based on the utilization of metal batch per operation, the filling percentage of the designed filling chamber and on the basis of the modification in the minimum required locking force of the machine. This assessment predicts the impact of gating system design method on the process and economic indicators but does not indicate the suitability of the design with respect to the quality of the cast. In this contribution, the hydrodynamic characteristics of melt flow are analytically performed on the already designed gating systems taken from [Majernikova 2024], based of which it is possible to assume the development of gas entrapment by the melt during its passage through the gating system. Subsequently, the assumption is verified using the MagmaSoft MAGMA 5.5.1 simulation program. One of the significant findings from calculations and resulting numerical simulations is the fact that within a certain range of the gating system geometry, the gas entrapment by the melt and their transport into the cast volume is mainly conditioned by the type of the melt flow in runners, and within another range of the gating system geometry, it is mainly conditioned by the filling mode of mold cavity. The optimal and therefore the lowest values of gas entrapment in the cast volume were achieved in the area of gating system geometric

characteristics with the achievement of advantageous ratios between the type of the melt flow and the filling mode of the mold cavity.

2 DESCRIPTION OF EXPERIMENTAL PROCEDURE

According to the gating system numerical design methodology used in [Majernikova 2024], five variants of gating systems were designed for a specific ty of electric motor flange cast, manufactured from alloy EN AC 47100 (Fig. 5).

Figure 5. Electric motor flange cast

Table 1 shows the basic volumetric and dimensional characteristics of the cast.

Table. 1 Volumetric and dimensional characteristics of the cast

Quantity	Value
Alloy	EN AC 47 100 – AlSi12Cu(Fe)
Alloy density ρ, kg.m^{-3}	2650
Cast volume Vcast, m^3	51697.9*10-9
Cast weight mC, kg	0.136
Cast diameter, m	0.1165
Characteristic cast wall thickness h_{CH}, m	0.002

2.1 Considered gating system

Based on variable input parameters and different formulations for determining the gate area, the geometric characteristics of the gates presented in Tab. 2 [Majernikova 2024] were achieved. As presented in [Majernikova 2024], the determination of the gating system channels cross-section depends on the gate cross-section. Tab. 3 shows the adopted and considered runners cross-sections.

When considering trapezoidal cross-section of the secondary runners, the dimensions of the runners for individual calculation variants are given in Tab. 4 [Majernikova 2024].

Table. 2 Gate dimensions

	Area of the Gate S_G	Length of the Gate a	Height of the Gate b, mm
Variant 1	S_{G1} = 76.06 mm^2	a = 60.968 mm	b_1 = 1.25 mm
Variant 2	S_{G2} = 48.32 mm^2	a = 60.968 mm	b_2 = 0.79 mm
Variant 3	S_{G3} = 119.50 mm^2	a = 60.968 mm	b_3 = 1.96 mm
Variant 4	S_{G4} = 66.05 mm^2	a = 60.968 mm	b_4 = 1.08 mm
Variant 5	S_{G5} = 35.03 mm^2	a = 60.968 mm	b_5 = 0.57 mm

Table. 3 Cross-section of the runners

	Cross-sectional area of the secondary runner	Cross-sectional area of the main runner
Variant 1	S_{SR1} = 228.18 mm^2	S_{MR1} = 501.99 mm^2
Variant 2	S_{SR2} = 144.96 mm^2	S_{MR2} = 318.91 mm^2
Variant 3	S_{SR3} = 358.50 mm^2	S_{MR3} = 788.70 mm^2
Variant 4	S_{SR4} = 198.15 mm^2	S_{MR4} = 435.92 mm^2
Variant 5	S_{SR5} = 105.09 mm^2	S_{MR5} = 231.20 mm^2

Table. 4 Runners geometric dimensions

	Variant 1	Variant 2	Variant 3	Variant 4	Variant 5
Secondary runner					
CT	11.48 mm	9.15 mm	14.39 mm	10.69 mm	7.79 mm
CB	22.96 mm	18.30 mm	28.78 mm	31.38 mm	15.58 mm
Main runner					
CT	11.48 mm	9.15 mm	14.39 mm	10.69 mm	7.79 mm
CB	46.80 mm	37.30 mm	58.66 mm	43.64 mm	31.80 mm
Curvature radius, r	6 mm	4.5 mm	7 mm	5 mm	4 mm

Wall inclination angle, α	75°	75°	75°	75°	75°

Since the methodology for designing the gating systems is being assessed, the length of the runners, their interconnection, and the overall shape of the gating system remained identical to the initial gating system used in real industrial production, with values l_{MR} = 264 mm and l_{SR}= 280 mm, by gating systems numerical design. Fig. 6 depicts the basic shape of the gating system and the casts distribution, including the filling chamber [Majernikova 2024].

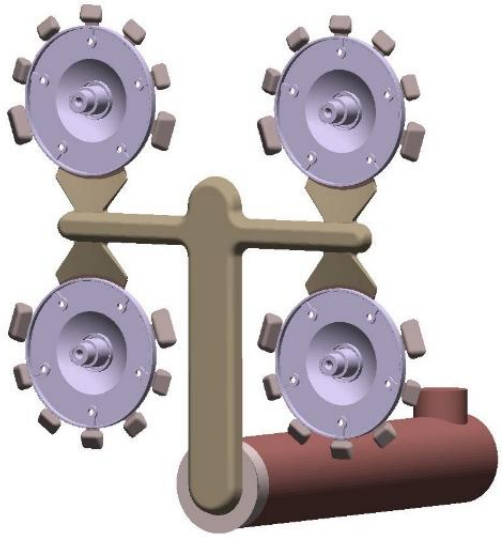

Figure 6. Basic shape of the gating system

2.2 Method for determining the hydrodynamic characteristics

Analytical assessment of gating system melt flow can be performed with respect to the type of melt flow in the gating system and the mold cavity filling mode. For this assessment, it is necessary to know the flowing melt velocity characteristics and the gating system individual parts geometry. To determine the runners theoretical velocity, it is possible to use the continuity equations (4), or their modified form according to the relation:

$$v_G * S_G = v_{SR/MR} * S_{SR/MR} \quad (4)$$

Where:

v_G – gate velocity [m.s^{-1}],

$v_{SR/MR}$ – velocity in the secondary/main runner [m.s^{-1}],

S_G – gate area [m^2].

$S_{SR/MR}$ – cross-sectional area of the secondary/main runner [m^2].

As mentioned in chapter 1 Introduction, in general, we distinguish between laminar flow, where the liquid flows without mixing of partial streams, and turbulent flow, where mixing of the partial streams occurs. The Reynolds number Re, determined according to the equation (1), serves as a partition coefficient to characterize the type of liquid flow in the runner. Since the cross-section of the runners is trapezoidal, to determine the average diameter of the pipe, it is necessary to consider the hydraulic diameter, determine according to the relation:

$$d_H = \frac{4*S_R}{P_R} \quad (5)$$

Where:

d_H – hydraulic diameter of the channel [m],

S_R – cross-sectional area of the gating channel [m^2].

P_R – channel circumference [m].

Hydraulic diameter is a length/dimensional characteristic of the stream flow cross-section. It expresses the equivalent cross-section replacement for pipes and channels of non-circular shape.

Based on the theoretical foundations of the mold cavity filling process with liquid metal developed by Frommer and Brandt (chapter 1 Introduction), it is possible to determine the mold cavity filling mode based on the partition coefficient determined by relations (2) and (3).

2.3 Assessment of gas entrapment using numerical simulations

The assessment of gas entrapment in casts at the end of the filling phase was performed using the Magmasoft MAGMA 5.5.1 program – HDPC module. The setting of the input parameters of the casting cycle and the casting process parameters was essentially identical to the casting machine settings when producing casts using the initial gating system. The differences between real casting and simulated casting are based on the calculation methodology. Based on the gating system design methodology and its numerical design presented in [Majernikova 2024], the melt velocity in gate was considered at a constant level v_G= 32.16 m.s^{-1}. The determination of the pressing piston velocity in the second phase v_{P2}, was based on the continuity equation, or rather its modified form according to the relation (6):

$$v_G * S_G = v_{P2} * S_P \quad (6)$$

Where :

v_G – gate velocity; v_G= 32.16 m.s^{-1},

v_{P2} – pressing piston velocity in second phase [m.s^{-1}],

S_G – gate area [m2]; variable according to Tab. 2,

S_P – pressing piston area; SP = 3.8465*10-3 m^2.

The determined values of the pressing piston velocity in the second phase are given in Tab. 5.

Table 5. Max. piston velocity in the second phase

Variant 1	v_{p2_1} = 2.54 m/s
Variant 2	v_{p2_2} = 1.62 m/s
Variant 3	v_{p2_3} = 4.00 m/s
Variant 4	v_{p2_4} = 2.21 m/s
Variant 5	v_{p2_5} = 1.17 m/s

The parameter settings for numerical simulation are given in Tab. 6.

To improve the simulation accuracy and to obtain a better description of the target entity, a mesh with high fineness and generation efficiency was chosen. A fine mesh was chosen for the casting cycle simulations, the parameters of which are stated in Tab. 7.

The assessment of gas entrapment in the cast volume was performed in the points where the cast is subsequently chipped and the occurrence of porosity in these points could be problematic during machining, with regard to the possibility of pores being exposed after chip removal. At the same time, these points were assessed as a critical with regard to the melt flow around the cores, which form a structural opening during casting. When the cores are flown around, two melt streams merge behind the core, which is rising the chances of further gas entrapment in the cast due to swirling and mixing of the melt. The assessed points are depicted in Fig. 7. The gas entrapment monitoring points in the melt volume are located 1 mm radially behind the core and 2 mm from cast surface into its volume. The monitoring points are designated SM1 to SM5 for each cast in the numbering sequence in the direction of rotation from SM1 to the axis of main runner.

The assessment of gas entrapment was performed using Air Entrapment submodule at the end of the filling time phase, i.e., at the moment when the gating system was filled to 100% of its volume just before the holding pressure phase. This moment was chosen taking into account that holding pressure largely eliminates the size and distribution of pores [Gaspar 2016]. Even in this moment, it is possible to evaluate only the proportion of gas entrapment into the cast volume due to the gating system geometry.

Table 6. Casting process parameters settings for numerical simulation

Technological parameters	
Parameter	**Value**
Alloy	EN AC 47 100 (AlSi12Cu1(Fe))
Melt temperature	708 °C
Die temperature	220 °C
Max. pressing piston velocity in the first phase	0.2 $m.s^{-1}$
Max. pressing piston velocity in the second phase	see *Tab. 5*
Holding pressure	25 MPa
Proces parameters	
Die treatment - spraying	Start – 5 s after cast removal
	Duration – 3 s
Die treatment - blowing	Start – 2 s after end of spraying
	Duration – 3 s
Die locking	2 s after end of blowing
Dosing	Start – 1 s after mold locking
	Metal batch volume [23] – Variant 1: 554.63*10^{-6} m^3
	– Variant 2: 490.12*10^{-6} m^3
	– Variant 3: 656.11*10^{-6} m^3
	– Variant 4: 536.92*10^{-6} m^3
	– Variant 5: 456.68*10^{-6} m^3
	Duration of batching – 5 s
	Delay – 3 s

Table 7. Mesh setting parameters

Element parameters			
	Element size, mm		
	In the x-axis direction	In the y-axis direction	In the z-axis direction
Mold	5	5	5
Runners	2	2	2
Tempering channels	2	2	2
Filling chamber + biscuit	2	2	2
Casts + overflows	0.66	0.33	0.66
Gate	0.38	0.19	0.38
***** cells are distributed equidistantly to the geometry of individual volumes			

Mesh parameters – total number of elements	
	Total number of elements in the mesh
Variant 1	121446920
Variant 2	121870080
Variant 3	123505920
Variant 4	121870080
Variant 5	121870080

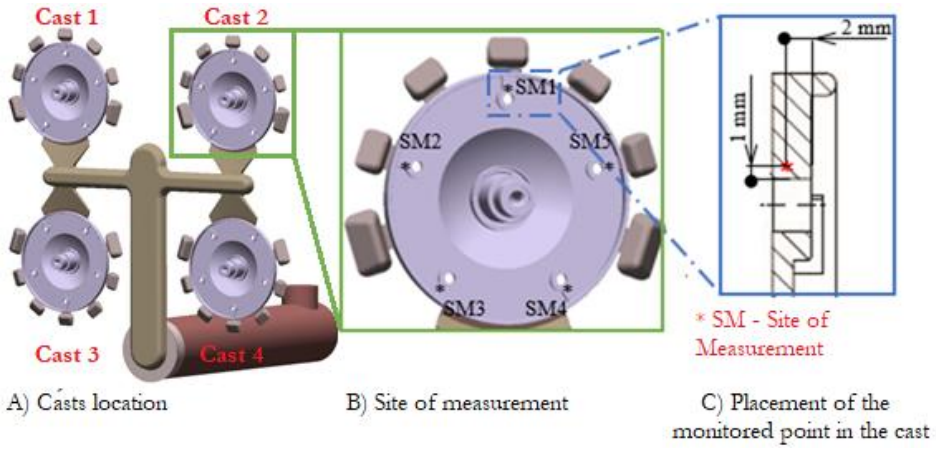

Figure 7. Monitored points for assessing the gas entrapment in cast volume

3 RESULTS

The assessment of high pressure die casting gating system numerical design methodology with regard to the material utilization will be performed in the following steps:

- determination of the melt flow velocity in runners,
- determination of the melt flow type in the runners,
- determination of the mold cavity filling mode,
- assessment of gas entrapment in the cast volume.

3.1 Determination of the melt flow velocity in runners

Based on the relation (4), the theoretical values of melt flow velocity in the runners for individual gating system designs are determined and are given in Tab. 8.

Table 8. Theoretical melt flow velocities in runners

	Velocity in main runner	Velocity in secondary runner
Variant 1	v_{MR1} = 19.46 m.s^{-1}	v_{SR1} = 21.41 m.s^{-1}
Variant 2	v_{MR2} = 19.54 m.s^{-1}	v_{SR2} = 21.49 m.s^{-1}
Variant 3	v_{MR3} = 19.50 m.s^{-1}	v_{SR3} = 21.46 m.s^{-1}
Variant 4	v_{MR4} = 19.50 m.s^{-1}	v_{SR4} = 21.45 m.s^{-1}
Variant 5	v_{MR5} = 19.47 m.s^{-1}	v_{SR5} = 21.41 m.s^{-1}

As follows from Tab. 8, the theoretical melt flow velocities in the runners for individual variants of gating system numerical designs acquire values that are almost constant. This phenomenon can be explained by the hypothesis of conservation of mass/volume flow velocity, from which it follows: If the flow velocity of the medium (melt) is preserved at the inlet and outlet, then the velocity characteristics of the medium when passing through the system with different cross-sections retain a constant character.

3.2 Determination of the melt flow type in the runners

Using the relations (1) and (5), substituting the values for individual variants of calculation and geometry of gating systems, the Reynolds number shown in Tab. 9 were determined.

Table 9. Determined of Reynolds number

	Variant 1	Variant 2	Variant 3	Variant 4	Variant 5
Secondary Runner					
d_{HSR}, mm	14.36	11.45	18.01	13.39	9.75
Re_{SR}	302177	240942	352293	281765	205169
Main Runner					
d_{HMR}, mm	18.05	14.39	22.63	16.82	12.24
Re_{MR}	344394	275267	432891	326208	234140

Based on the data stated in Tab. 9, it can be assumed that with increasing of hydraulic cross-section, or with increasing the cross-section of the runners area, the value of the Reynolds number increases, which allows us to conclude that there is higher turbulence in the melt flow through the runners. This fact is conditioned by the fact that if the constant flow velocity is maintained when the hydraulic cross-section d_H is increased (Tab. 8), Reynolds number Re will increase, and thus the turbulence in the flowing melt also increases.

3.3 Determination of the mold cavity filling mode

Based on the theoretical foundations of the mold filling with liquid metal developed by Frommer and Brandt, it is possible to determine the mold cavity filling mode based on distribution coefficient determine by relations (2) and (3). The values of the SG/SC are stated in Tab. 10.

Table 10. Determined of the mold cavity filling mode

	Ratio S_G/S_C	Filling mode
Variant 1	0.124	According to Frommer

Variant 2	0.079	According to Frommer
Variant 3	0.195	According to Frommer
Variant 4	0.108	According to Frommer
Variant 5	0.057	According to Frommer

On the basis of data, it is possible to assume that the mold cavity filling will proceed in the Frommer mode. At the same time, it is possible to express the opinion that with a decreasing S_G/S_C ratio and therefore with decreasing area of the gate, the emergence of a disperse melt flow in the mold cavity will be more pronounced.

3.4 Assessment of gas entrapment in cast volume

The measured values of the proportion of gas entrapment in cast volume at the monitored points according to Fig. 7 are stated Tab. 11 - Tab. 15.

Table 11. Gas entrapment ic cast volume for Variant 1

	SM1	SM2	SM3	SM4	SM5	Average
Cast 1	0.303 %	0.002 %	0.017 %	0.032 %	0.001 %	0.071 %
Cast 2	1.170 %	0.007 %	0.018 %	0.038 %	0.004 %	0.247 %
Cast 3	0.154 %	0.002 %	0.003 %	0.028 %	0.002 %	0.038 %
Cast 4	0.725 %	0.000 %	0.002 %	0.031 %	0.000 %	0.154 %
					Total Avg.	0.127 %

Table 12. Gas entrapment ic cast volume for Variant 2

	SM1	SM2	SM3	SM4	SM5	Average
Cast 1	1.840 %	0.004 %	0.011 %	0.129 %	0.000 %	0.397 %
Cast 2	1.849 %	0.017 %	0.098 %	0.399 %	0.000 %	0,399 %
Cast 3	2.450 %	0.006 %	0.026 %	0.598 %	0.003 %	0.617 %
Cast 4	1.425 %	0.009 %	0.120 %	0.236 %	0.001 %	0.358 %
					Total Avg.	0.443 %

Table 13. Gas entrapment ic cast volume for Variant 3

	SM1	SM2	SM3	SM4	SM5	Average
Cast 1	2.201 %	0.007 %	0.114 %	0.163 %	0.015 %	0.500 %
Cast 2	0.164 %	0.011 %	0.030 %	0.046 %	0.000 %	0.050 %
Cast 3	2.799 %	0.004 %	0.061 %	0.072 %	0.002 %	0.588 %
Cast 4	2.499 %	0.007 %	0.023 %	0.126 %	0.004 %	0.532 %
					Total Avg.	0.417 %

Table 14. Gas entrapment ic cast volume for Variant 4

	SM1	SM2	SM3	SM4	SM5	Average
Cast 1	1.917 %	0.006 %	0.007 %	0.334 %	0.001 %	0.453 %
Cast 2	0.666 %	0.000 %	0.006 %	0.010 %	0.000 %	0.136 %
Cast 3	1.246 %	0.002 %	0.003 %	0.224 %	0.002 %	0.295 %
Cast 4	0.289 %	0.004 %	0.025 %	0.029 %	0.000 %	0.069 %
					Total Avg.	0.239 %

Table 15. Gas entrapment ic cast volume for Variant 5

	SM1	SM2	SM3	SM4	SM5	Average
Cast 1	0.060 %	0.000 %	0.000 %	0.043 %	0.000 %	0.021 %
Cast 2	3.333 %	0.206 %	0.690 %	1.417 %	0.031 %	1.135 %
Cast 3	2.925 %	0.003 %	0.007 %	0.100 %	0.000 %	0.607 %
Cast 4	3.129 %	0.000 %	0.008 %	0.011 %	0.000 %	0.630 %
					Total Avg.	0.598 %

From data stated in Tab. 11 to Tab. 15, and according to the layout of monitored points from Fig. 7, it can be seen that when comparing the proportions of gas entrapment in individual locations of the cast, the highest proportion of gas entrapment is in the area around points SM1, followed by SM4 and SM3. This gas congestion correlates with the mold cavity filling mode, which is managed by the Frommer mode. After the melt flow passes through the mold cavity, the area around point SM1 is the first to be supplied by the melt, which means that the overflow subsequent to this area is also filled first. Its filling eliminates its function and effective removal of gases from the melt to this area, in which the melt is still flowing. Points SM4 and SM3 are located in the area closest to the gate. Thus, between the gate and point SM4/SM3, there are no longer dimensioned any

overflows and effective venting, which is associated with a higher proportion of gas entrapment in the cast volume. Based on the above, it can be stated that the gas entrapment in the cast volume is not only related to the factors supporting the distribution of the gases into mold cavity, but also to the effective and functional venting of the mold and the layout of venting channels.

4 DISCUSSION

The contribution develops the conclusions from the article Methodology assessment of the gating system numerical design of high pressure die casting with regard to the material applicability [Majernikova 2024], from which it takes over the considered gating system geometries designed according to various numerical design formulations. In this contribution, the hydrodynamic characteristics of the melt flow are analytically converted, based on which it is possible to predict the development of gas entrapment by the melt during its passage through the gating system.

The analytical assessment of the gating system melt flow was aimed at assessing the type of melt flow in the runners and assessing the mold cavity filling mode. To evaluate the hydrodynamic conditions in the gating system, it was necessary to determine the theoretical melt flow velocity characteristics, The theoretical melt flow velocities (Tab. 8) were determined using the continuity equation, relating them to the melt velocity in gate and its cross-section. It was determined that the melt flow velocities reached a relatively constant level in all calculation variants. This fact can be justified by the hypothesis of the conservation of mass/volume flow. It follows from this that as long as the melt flow velocity is maintained, whether volumetric or mass, at inlet and outlet, the velocity characteristics of the melt when passing through the gating system with different cross-sections show a constant character.

To determine the flow type in runners, turbulent flow was assumed. This assumption was confirmed by calculating the Reynolds number. It was found that with an increasing runners cross-section, the Reynolds number also increases, and therefore the turbulence of the flow increases (Tab. 9). Although increasing the runners cross-section may seem like a way to reduce the turbulence, the opposite is true. The Reynolds number would decrease with an increase in the cross-section only if a constant flow rate at the inlet was maintained, thereby reducing the velocity in the channel. However, if constant velocity is maintained when the cross-section is modified, the Reynolds number increases. As follows from the theory of foundry, the runners flow type is determined by the velocity of the melt stream. As the melt flow velocity increases, the turbulence in its stream increases. If it is necessary to maintain the flow velocity, or if it is not possible to reduce the velocity from a technological point of view, the way to reduce the turbulence in the melt stream while maintaining the flow rate is to divide the runners, which was confirmed by comparing the Reynolds number between the main and the secondary runner in Tab. 9 and Fig. 8.

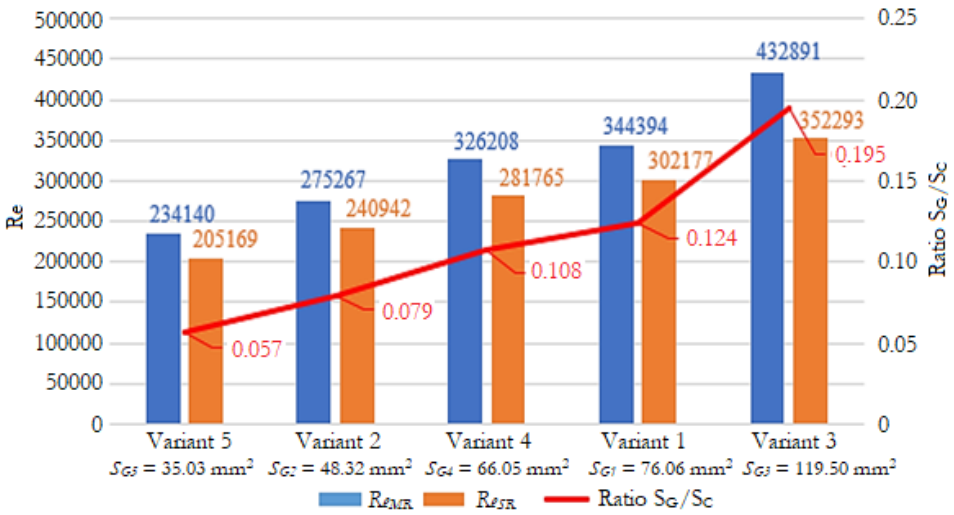

Figure 8 Dependence of the melt flow type and mode on the gate cross-section

Based on the results stated in Tab. 2, Tab. 9 and Tab. 10, a graph of dependence of melt flow type in runners and mold cavity filling mode on the gate cross-section was constructed, as depicted in Fig. 8. As arises from the Fig. 8, with an increasing gate cross-section, which is determined by the runners cross-section, the value of the Reynolds number Re increases, which gives the assumption of an increase in turbulence in melt when passing through the runners. Based on this state, it is possible to predict an increased proportion of gas entrapment by the melt, which will be transported into the cast. In contrast, with an increasing value of the gate cross-section S_G, the S_G/S_C ration also increases, which gives the assumption of a calmer mold cavity filling and more consistent melt flow when passing through the mold cavity past the gate. Which of the above-mentioned aspects of the hydrodynamic melt flow assessment is limiting for gas entrapment in the cast volume is assessed using numerical simulations.

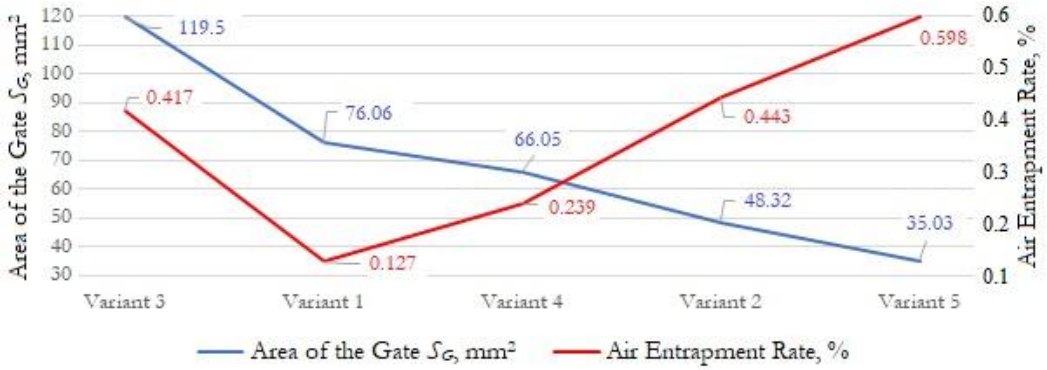

Figure 9. Gas entrapment dependence on the gate cross-section

According to the average values of cast volume gas entrapment for individual variants (Tab. 11 – Tab. 15), a graph of the gas entrapment dependence on the gate cross-section was constructed, depicted in Fig. 9. As its evident in the figure, with a decreasing gate cross-section value, the value of cast volume gas entrapment increases. Variant 3 forms a certain extreme, because at the largest gate cross-section an increase in gas entrapment occurs. An explanation can be sought in Fig. 8 and Tab. 9, from which it is evident that the Re values are at highest in Variant 3, which determines the most turbulent melt flow in runners. Therefore, it can be assumed that in Variant 3, turbulent flow in runners has the majority proportion of gas distribution in the cast volume. For other Variants 1, 2, 4, 5, the determining parameter will be the S_G/S_C ratio, in which, with its decreasing value, the dispersive nature of the flow prevails, and thus the gas entrapment conditions in the cast volume are more suitable.

Considering the measured values of cast volume gas entrapment, which were obtained using numerical simulation (Fig. 9 and Tab. 11 - Tab. 15) and its comparing with the Reynolds number values and S_G/S_C ratio, as depicted in Fig. 10, we can partially explain the linearity extremes of gas entrapment process, which was assumed based on the casting theory and from experimental conclusions of the publications in the cited literature.

Figure 10. Flow and gas entrapment characteristics comparison in the melt

It is possible to assume that in individual calculation variants of the gating system and its design solutions, the major influence of the mold cavity gas entrapment by the melt alternates between turbulence caused by the Reynolds number Re and dispersion derived from the S_G/S_C ratio. Therefore, respecting the gate cross-section and the S_G/S_C ratio, it is possible to assume that the graph area can be divided into three areas:

I. area where the cast volume gas entrapment is mainly influenced by the Reynolds number Re, i.e. by the turbulence of the melt during its passage through the runners;
II. area of favorable ratios between Re and SG/SC, i.e. between the melt flow type in the runners and the mold cavity filling mode;
III. area where the cast volume gas entrapment in mainly influenced by the SG/SC ratio value.

In connection with the above statement, it would be appropriate to focus further research on the melt velocity and pressure ratios assessment in the area before and past the gate, while modifying the mutual ratios of Re and S_G/S_C for a wider range of casts and gating systems.

When assessing the cast volume gas entrapment using numerical simulation, a slight zonation in the cast volume gas entrapment was detected. This is related to the mold cavity filling mode and the overflows distribution. Higher cast volume gas entrapment values were detected at the point SM1 located opposite to the gate, and subsequently at points SM3 and SM4 located in the gate area. The higher gas entrapment proportion in the area around SM1 can be explained by the rapid filling of the overflow past the measured point SM1, thereby eliminating this overflow from its function. Points SM3 and SM4 are located in the area near the gate, which is filled last, and therefore gases are trapped in this area without the possibility of discharge through the venting system. It is appropriate to focus on the design and layout of the overflows in the further research of the problem. It would be appropriate to place an overflow with a larger volume in the measured point SM1 area and to add additional overflows in the measured points SM3 and SM4 areas.

5 CONCLUSIONS

The presented contribution is focused on assessing the suitability of the gating system design numerical method for a specific type of low-weight silumin cast produced by the high-pressure die casting technology. Based on the performed calculations, assessment of the melt flow hydrodynamic characteristics in the designed gating systems, the use of numerical simulations using the MagmaSoft software, as well as mutual comparison of the above-mentioned partial factors, the following conclusions can be drawn:

- by determination of melt velocity (Tab. 8) in the runners, the hypothesis of maintaining the mass/volume flow rate of such a melt was verified, which implies that when maintaining the mass/volume flow melt velocity in the channels, the flow velocity does not change due to the channels geometry;
- When maintaining the mass/volume flow rate and therefore the relatively constant velocity in the channels, with increasing the runner cross-section S_{MR} and S_{SR}, the Reynolds number value Re increases (Tab. 9), which causes a higher melt flow turbulence degree. From this, it can be concluded that there is a higher melt volume gas entrapment proportion;
- the S_G/S_C ratio increases with increasing the SG value (Tab. 10). A higher ration determines a calmer mold cavity filling mode with melt. From this, it can be concluded that the melt volume gas entrapment proportion is lower;
- assessing the cast volume gas entrapment values according to Tab. 11 - Tab. 15 (Fig. 9) and its comparison with the statements in the previous points, three characteristics of majority influence of gas entrapment and gas distribution into the cast volume were defined in accordance with Fig. 10 for the gating systems dimensions calculation, depending on the flow hydrodynamic characteristics, as stated in Chapter 4.

If we consider the gas entrapment by the melt and their distribution in the cast volume as the determining parameter, which is assessed by the Air Entrapment module, then the most advantageous gating system variant for an electric motor flange production according to Fig. 5 and Fig. 6 is Variant 1. Since the article is based on the assumptions and follows the conclusions presented in the publication Methodology assessment of the gating system numerical design of high pressure die casting with regard to the material applicability [Majernikova 2024], it is necessary to consider the indicators considered also in this publication [Majernikova 2024] when assessing the overall suitability of the gating systems numerical design methodology. The final assessment resulting from the publication [Majernikova 2024] and the conclusions from it can be marked with regard to the speed and simplicity of the gate cross-section S_G calculation, the numerical method according to the Variant 4. Even though in Variant 1 the cast volume gas entrapment values in the monitored points were at the lowest level, considering the metal applicability as an economic indicator, the technological parameter of the locking force intensity, and the area of advantageous ratios of Re and S_G/S_C defined in Fig. 10, the best calculation and design results from the intersection of these quantities are according to Variant 4.

With reference to Fig. 10 and the definition of the areas with a conditional major influence of the cast volume gas entrapment mechanism, it is necessary to focus on the area of favorable Re and S_G/S_C ratios. As mentioned above, this assumption must be verified on a wider range of casts and gating systems designs. Subsequently, it is necessary to consider the fact that Re can be influenced by the melt flow velocity at a constant gating system geometry. The gas entrapment by the melt is also conditioned by the filling percentage of the filling chamber with the melt, as well as by the pressing piston velocity in the first phase of pressing and the pressing piston velocity ration in the first and second phases. These aspects will be investigated in the following research activities.

REFERENCES

[Bate 2023] Bate, C., King, P., Sim, J., et al. A Novel Approach to Visualize Liquid Aluminum Flow to Advance Casting Science. Materials, 2023, Vol. 16, No. 2, Art. No. 756. DOI: 10.3390/ma16020756.

[Bolibruchova 2019] Bolibruchova, D., Matejka, M., Kuris, M. Analysis of the impact of the change of primary and secondary AlSi9Cu3 alloy ratio in the batch on its performance. Manufacturing Technology, 2019, Vol. 19, No. 5, pp 734-739. DOI: 10.21062/ujep/367.2019/a/1213-2489/MT/19/5/734.

[Cao 2019] Cao, H., Shen, Ch., Wang, Ch., et al. Direct observation of filling process and porosity prediction in high pressure die casting. Materials, 2019, Vol. 12, No. 7, Art. No. 099. DOI: 10.3390/ma12071099.

[Cao 2020] Cao, H., Luo, Z., Wang, Ch., et al. The stress concentration mechanism of pores affecting the tensile properties in vacuum die casting metals. Materials, 2020, Vol. 13, No. 13, Art. No. 3019. DOI: 10.3390/ma13133019.

[Damle 1996] Damle, Ch., Sahai, Y. A Criterion for Water Modeling of non-isothermal Melt Flows in Continuous Casting Tundishes. ISIJ International, 1996, Vol. 36, No. 6, pp. 681-689. ISSN 0915-1559. DOI: 10.2355/isijinternational.36.681.

[Duan 2023] Duan, Z., Chen, W., Pei, X., et al. A multimodal data-driven design of low pressure die casting gating system for aluminum alloy cabin. J. of Materials Research and Technology, 2023, Vol. 27, No. November 2023, pp. 2723-2736. ISSN 2238-7854. DOI: 10.1016/j.jmrt.2023.10.076.

[Dybalska 2021] Dybalska, A., Caden, A., Griffiths, W.D., et al. Enhancement of mechanical properties of pure aluminium through contactless melt sonicating treatment. Materials, 2021, Vol. 14, No. 16, Art. No. 4479. DOI: 10.3390/ma14164479.

[Gaspar 2016] Gaspar, S., Pasko, J. Pressing Speed, Specific Pressure and Mechanical Properties of Aluminium Cast. Archives of Foundry Engineering, 2016, Vol. 2016, No. 2, pp 45-50. DOI: 10.1515/afe-2016-0024.

[Gaspar 2019] Gaspar, S., Pasko, J. Plunger pressing speed like the main factor influencing of the mechanical properties of die casting. MM Science Journal, 2019, Vol. 2019, No. December, pp. 3490–3493. ISSN 1803-1269. DOI: 10.17973/MMSJ.2019_12_2019029.

[Kuznetsov 2020] Kuznetsov, E., Nahornyi, V., Krenicky, T. Gas Flow Simulation in The Working Gap of Impulse Gas-barrier Face Seal. Management Systems in Production Engineering, 2020, Vol. 28, No. 4, pp. 298-303.

[Majidi 2019] Majidi, S.H., Beckermann, C. Effect of Pouring Conditions and Gating System Design on Air Entrainment During Mold Filling. International J. of Metalcasting, 2019, Vol. 13, No. 2, pp. 255-272. DOI: 10.1007/s40962-018-0272-x.

[Majernik 2019] Majernik, J., Podaril, M. Influence of runner geometry on the gas entrapment in volume of pressure die cast. Archives of Foundry Engineering, 2019, Vol. 19, No. 3, pp. 33-38. DOI: 10.24425/afe.2019.129626.

[Majernik 2024] Majernikova, M., Majernik, J., Podaril, M., et al. Methodology assessment of the gating system numerical design of high-pressure die casting with regard to the material applicability. MM Science Journal, 2024, Vol. 2024, No. December, pp. 8033-8043. DOI: 10.17973/MMSJ.2024_12_2024108.

[Novakova 2017] Novakova, I., Moravec, J., Kejzlar, P. Metallurgy of the Aluminium Alloys for High-Pressure Die Casting. Manufacturing Technology, 2017, Vol. 17, No. 5, pp. 804-811. ISSN 1213-2489.

[Otsuka 2014] Otsuka Y. Experimental verification and accuracy improvement of gas entrapment and shrinkage porosity simulation in high pressure die casting process. Materials Transact., 2014, Vol. 55, No. 1, pp. 154-160. DOI: 10.2320/matertrans.F-M2013835.

[Pasko 2014] Pasko, J., Gaspar, S., Technological Factors of Die Casting. Ludenscheid: RAM-Verlag, 2014. ISBN 978-3-942303-25-5.

[Ragan 2007] Ragan, E., et al. High Pressure Die Casting (Liatie kovov pod tlakom). Presov: FMT TUKE, 2007. ISBN 978-80-8073-979-9.

[Ruzbarsky 2014] Ruzbarsky, J., Pasko, J., Gaspar, S. Techniques of Die Casting. Ludenscheid: RAM-Verlag, 2014. ISBN 978-3-942303-29-3.

[Sahai 1996] Sahai, Y., Emi, T. Criteria for Water Modeling of Melt in Continuous Casting Tundishes. ISIJ International, 1996, Vol. 36, No. 9, pp. 1166-1173. DOI: 10.2355/isijinternational.36.1166.

[Serak 2020] Serak, J., Vojtech, D., Simon, C. The Influence of Thermal History on the Microstructure and Mechanical Properties of AlSi8Cu2Fe Alloy. Manufacturing Technology, 2020, Vol. 20, No. 4, pp. 521-526. DOI: 10.21062/mft.2020.071.

[Tavodova 2022] Tavodova, M., Vargova, M., Stancekova, D., et al. Evaluation of the Influence of Process Parameters on the Mechanical Properties of Castings during High Pressure Die Casting. Manufacturing Technology, 2022, Vol. 22, No. 6, pp. 764-770. DOI: 10.21062/mft.2022.079.

[Uhricik 2017] Uhricik, M., et al. The Structure of the Aluminium Alloy and Its Influence on the Fatigue Properties. Manufacturing Technology, 2017, Vol. 17, No. 5, pp. 863-869. ISSN 1213-2489.

[Vlach 2022] Vlach, T., Cais, J. The Effect of Casting Mold Material on Microstructure of Al-Si Alloys. Manufacturing Technology, 2022, Vol. 22, No. 5, pp. 617-623. DOI: 10.21062/mft.2022.072.

[Zhao 2018] Zhao, X., Wang, P., Li, T., et al. Gating system optimalization of high pressure die casting thin-wall AlSi10MnMg longitudinal loadbearing beam based on numerical simulation. China Foundry, Vol. 15, No. 6, pp. 436-442. DOI: 10.1007/s41230-018-8052-z.

CONTACTS:

Ing. Jan Majernik, PhD.
The Institute of Technology and Business in Ceske Budejovice
Faculty of Technology Department of Mechanical Engineering
Okruzni 517/10, 370 01 Ceske Budejovice, Czech Republic
+420 387 842 137, majernik@mail.vstecb.cz , https://is.vstecb.cz/osoba/majernik

University of South Bohemia in Ceske Budejovice
Faculty of Agriculture and Technology
Studentska 1668, 370 05 Ceske Budejovice. Czech Republic
jmajernik@jcu.cz